

Hedgehog pathway inhibitor saridegib (IPI-926) increases lifespan in a mouse medulloblastoma model

Michelle J. Lee^{a,b,1}, Beryl A. Hatton^{a,1}, Elisabeth H. Villavicencio^{a,c}, Paritosh C. Khanna^d, Seth D. Friedman^d, Sally Ditzler^a, Barbara Pullar^a, Keith Robison^e, Kerry F. White^e, Chris Tunkey^e, Michael LeBlanc^f, Julie Randolph-Habecker^g, Sue E. Knoblauch^g, Stacey Hansen^a, Andrew Richards^a, Brandon J. Wainwright^h, Karen McGovern^e, and James M. Olson^{a,b,c,2}

^aClinical Research Division, ^fPublic Health Sciences Division, ^gComparative Medicine, Fred Hutchinson Cancer Research Center, Seattle, WA 98109; ^bNeurobiology and Behavior Program, Departments of ^dRadiology and ^ePediatrics, University of Washington and Seattle Children's Hospital, Seattle, WA 98105; ^cInfinity Pharmaceuticals, Cambridge, MA 02139; and ^hDivision of Molecular Genetics and Development, Institute for Molecular Biosciences, University of Queensland, Brisbane QLD 4072, Australia

Edited by Dennis A. Carson, University of California at San Diego, La Jolla, CA, and approved April 4, 2012 (received for review September 13, 2011)

The Sonic Hedgehog (Shh) pathway drives a subset of medulloblastomas, a malignant neuroectodermal brain cancer, and other cancers. Small-molecule Shh pathway inhibitors have induced tumor regression in mice and patients with medulloblastoma; however, drug resistance rapidly emerges, in some cases via de novo mutation of the drug target. Here we assess the response and resistance mechanisms to the natural product derivative saridegib in an aggressive Shh-driven mouse medulloblastoma model. In this model, saridegib treatment induced tumor reduction and significantly prolonged survival. Furthermore, the effect of saridegib on tumor-initiating capacity was demonstrated by reduced tumor incidence, slower growth, and spontaneous tumor regression that occurred in allografts generated from previously treated autochthonous medulloblastomas compared with those from untreated donors. Saridegib, a known P-glycoprotein (Pgp) substrate, induced Pgp activity in treated tumors, which likely contributed to emergence of drug resistance. Unlike other Smoothed (Smo) inhibitors, the drug resistance was neither mutation-dependent nor *Gli2* amplification-dependent, and saridegib was found to be active in cells with the D473H point mutation that rendered them resistant to another Smo inhibitor, GDC-0449. The fivefold increase in lifespan in mice treated with saridegib as a single agent compares favorably with both targeted and cytotoxic therapies. The absence of genetic mutations that confer resistance distinguishes saridegib from other Smo inhibitors.

Medulloblastoma is the most common malignant brain cancer in children. Although long-term survival for standard- and high-risk medulloblastoma patients is now greater than 70% and 50%, respectively, it comes at a significant cost of toxicity because of surgery, radiation, and chemotherapy (1). Sonic Hedgehog (Shh) pathway activation represents ~20–25% of all medulloblastoma cases. Shh pathway activation also drives several other types of cancer through cell-autonomous oncogenic mechanisms or induction of microenvironment properties that provide a growth advantage to tumor cells (2). Therefore, pathway inhibitors are being actively investigated for Shh-driven cancers.

Current drugs in development primarily target the Smoothed (Smo) protein. In normal Shh signaling, Smo is released from inhibition by the Patched (Ptch) receptor by surface binding of Shh. Smo then activates downstream Shh targets such as the Gli transcription factors. HhAntag, the first synthetic small-molecule Smo antagonist reported, induces resolution of autochthonous brain tumors and flank medulloblastoma xenografts in the *Ptch1*^{+/-}; *p53*^{-/-} mouse model (3). Newer-generation synthetic small molecules targeting the Smo protein are now being used in patients. GDC-0449 (vismodegib) was reported to induce significant reduction in tumor burden in an adult Shh-driven medulloblastoma patient (4). Although these were important first steps toward effectively targeting the Shh pathway in cancer, responses were pronounced yet short-lived because of the emergence of

drug resistance (4–6). It remains to be determined whether these drugs confer a survival benefit to medulloblastoma patients. The identification of Smo inhibitors that remain active against cells that develop resistance to other agents in this class could benefit patients, particularly if acquired resistance is limited or slower to develop.

Saridegib is a unique, selective, and potent small molecule that targets the Shh pathway by inhibiting Smo. Saridegib is orally bioavailable and has demonstrated biological activity in multiple preclinical animal models of cancer (7). In a phase I study with saridegib, encouraging evidence of clinical activity was observed. In the current study, we assessed saridegib activity in an aggressive mouse medulloblastoma model, the conditional *Ptch1*-null (hereafter referred to as *Ptc*^{C/C}), that lacks both alleles of *Ptch1* specifically in cerebellar granule neuron precursors (8). The *Ptc*^{C/C} model is notable for massive hyperproliferation of granule cells throughout the cerebellum and the evolution of highly aggressive tumors that are clinically evident as early as postnatal day (P)21 and induce death within weeks after mice become symptomatic.

With few exceptions, targeted therapies have been disappointing in human clinical trials, largely because of rapid emergence of resistance mutations. In this study, we evaluated the efficacy of saridegib in a highly aggressive medulloblastoma model and evaluated drug resistance with particular attention to cell-autonomous point mutations or amplifications that confer resistance to other agents. Here, we showed that drug resistance observed after extended treatment periods is primarily caused by increased expression and activity of P-glycoprotein (Pgp) drug transporter rather than the emergence of genetic mutations that prevent drug–target interactions.

Results

Saridegib Induces Clinical Remission and Extends Survival. We performed a pilot study to evaluate the efficacy of saridegib in 21-day-old *Ptc*^{C/C} mice with clinical evidence of medulloblastoma. Mice

Author contributions: M.J.L., B.A.H., E.H.V., S.D., B.P., and J.M.O. designed research; M.J.L., B.A.H., E.H.V., P.C.K., S.D.F., S.D., B.P., K.R., K.F.W., C.T., S.E.K., S.H., A.R., and K.M. performed research; M.J.L., B.A.H., P.C.K., S.D., B.P., K.R., K.F.W., C.T., J.R.-H., S.E.K., B.J.W., K.M., and J.M.O. contributed new reagents/analytic tools; M.J.L., B.A.H., P.C.K., M.L., K.M., and J.M.O. analyzed data; and M.J.L., B.A.H., and J.M.O. wrote the paper.

Conflict of interest statement: Infinity Pharmaceuticals provided saridegib and partial funding for the studies as well as performed HPLC/MS analysis to measure drug concentrations and DNA sequencing analyses in samples provided to them. However, the company did not have a role in designing the studies, collecting samples, or drawing conclusions.

This article is a PNAS Direct Submission.

Data deposition: The data reported in this paper have been deposited in the Gene Expression Omnibus (GEO) database, www.ncbi.nlm.nih.gov/geo (accession no. GSE37417).

¹M.J.L. and B.A.H. contributed equally to this work.

²To whom correspondence should be addressed. E-mail: olson@fhcrc.org.

This article contains supporting information online at www.pnas.org/lookup/suppl/doi:10.1073/pnas.1114718109/-DCSupplemental.

were randomized to receive either daily i.p. saridegib (20 mg/kg per dose, $n = 3$) or vehicle ($n = 2$) for 19 d. Full resolution of clinical symptoms was evident by 19 d of treatment (Fig. 1A). In contrast, vehicle-treated mice showed progressive tumor growth. Analysis of gross tumor pathology after treatment demonstrated a strong response to saridegib therapy, with decreased cerebellar tumor size in treated mice (Fig. 1B). Imaging with Tumor Paint (chlorotoxin: Cy5.5), a tumor-tracking molecular bioconjugate (9), showed a reduction in tumor burden in saridegib-treated mice (Fig. 1C), and histopathological analysis of cerebellar tumor sections also revealed a decrease in tumor burden (Fig. 1D). The foliation pattern in the cerebellum was completely obliterated in vehicle-treated tumors, whereas saridegib-treated animals manifested regions of tumor cell death, as indicated by pyknotic nuclei with retention of normal cerebellar architecture. Given these promising results, we performed a larger-scale study and extended the duration of therapy. Study animals received 6 wk of daily saridegib ($n = 26$) versus vehicle control ($n = 11$). Three- to five-week-old mice with tumors were randomized to receive daily saridegib (20 mg/kg per dose) or vehicle. Kaplan–Meier analysis demonstrated that all mice treated with daily saridegib for 6 wk (Fig. 2, dashed line) survived, whereas all vehicle-treated mice (Fig. 2, solid line) developed ataxia and neurologic deficits and eventually succumbed to their disease ($P < 0.001$). Clinical symptoms were resolved in many of the saridegib-treated mice, accompanied by restored neurologic function and increased activity. The profound difference between 100% survival and neurologic recovery in saridegib-treated mice compared with 100% death in vehicle-treated mice prompted in-depth analyses of tumor response.

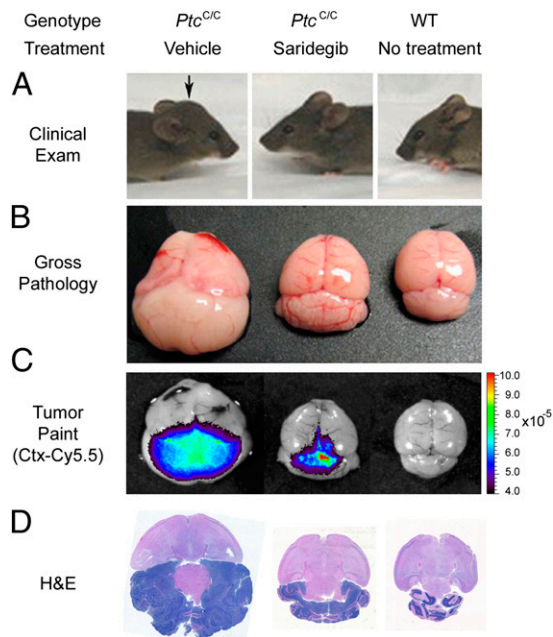


Fig. 1. The Smo inhibitor saridegib causes regression of mouse medulloblastoma and resolution of advanced clinical symptoms. Three-week-old mice symptomatic for medulloblastoma were randomized to receive daily i.p. saridegib (20 mg/kg per dose, $n = 3$) or vehicle ($n = 2$) for 19 d. (A) Compared with a representative vehicle-treated mouse with a large tumor (Left) and a WT littermate with no tumor (Right), a representative mouse treated with saridegib (Center) showed complete resolution of clinical symptoms after 19 d of saridegib treatment. Arrow denotes the bulging skull caused by tumor. (B–D) Response to saridegib was apparent by gross pathology (B), imaging with Tumor Paint (chlorotoxin: Cy5.5) (C), and H&E staining (D).

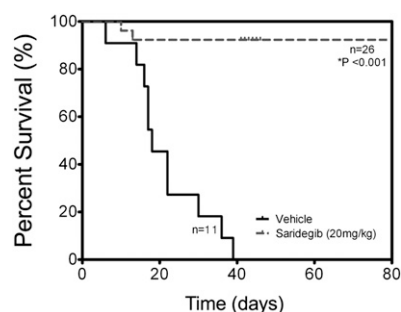


Fig. 2. Saridegib improves survival in the $Ptc^{C/C}$ medulloblastoma model. Kaplan–Meier analysis demonstrates that all $Ptc^{C/C}$ mice receiving daily saridegib (20 mg/kg, dashed line) survived, whereas all vehicle-treated mice (solid line) succumbed to their disease before the 6-wk time point ($P < 0.001$).

MRI Detects Subclinical Disease Progression. By using a technique that preserved intracerebral architecture, histological findings were compared with MRI findings in mice that were euthanized within days of an MRI (Fig. 3). Histopathological evaluation of tumors treated with saridegib for 6 wk showed reduced tumor volume and a moderate reduction in tumor cell density. Extending these findings noninvasively, MRI analyses at 3-wk intervals showed that saridegib treatment induced substantial tumor regression after 3 wk of daily administration (Fig. 4). Hydrocephalus, enlarged ventricles (Fig. 4A, yellow arrow), and transependymal cerebral spinal fluid (CSF) flow (Fig. 4A, red arrow) were commonly noted in vehicle-treated mice and were minimal in drug-treated mice (Fig. 4A and Fig. S1). Mice treated with saridegib showed a reduction of $Ki67^+$ cells in tumor after 4 d of treatment (Fig. S2), indicating an arrest of cell proliferation. Nevertheless, approximately half of the mice treated with saridegib (20 mg/kg per d) exhibited a rebound in tumor growth by 6 wk after maximal size reduction at 3 wk (Fig. 4B and C).

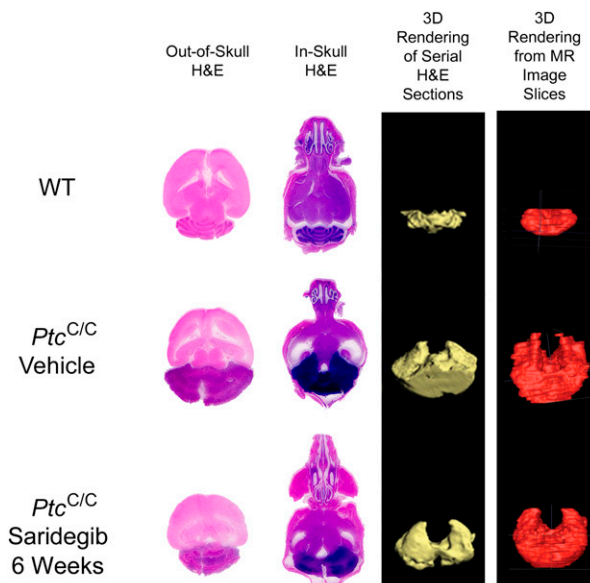


Fig. 3. In-skull tissue processing preserves intracranial integrity, enabling accurate 3D tumor volume rendering and analysis of pathology. Image panel summarizing a comparison of tissue sections from brains processed outside of (first column) or from within (second column) the skull and the related H&E-based 3D renderings (third column) of cerebellar or tumor volume. H&E-based 3D tumor models are matched to the MRI-generated volume model (fourth column) for the same sample.

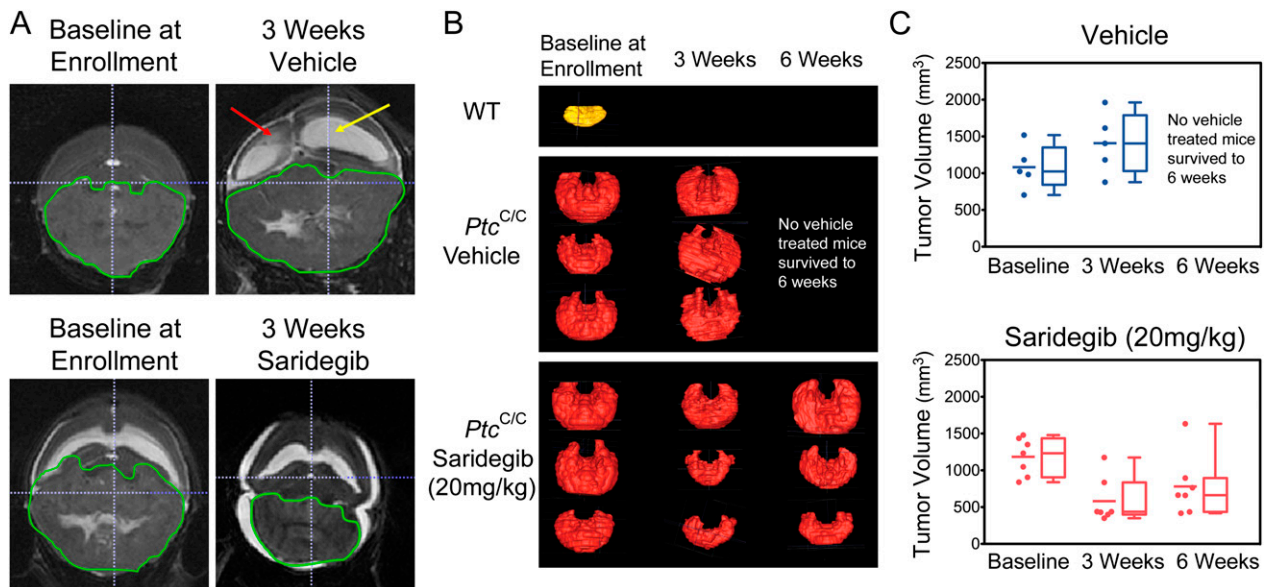


Fig. 4. MRI scans demonstrate decreasing tumor volumes at multiple treatment time points during daily saridegib administration but indicate tumor progression despite prolonged therapy. (A) A representative T2-weighted MRI image demonstrates the enlarged ventricles (yellow arrow) and transpendymal CSF flow (red arrow) resulting from cerebellar tumor progression in a vehicle-treated mouse. Saridegib-treated mice demonstrate a significant reduction in ventricle size and a resolution of transpendymal CSF flow. (B) Tumor volume was estimated from MRI scans taken at enrollment, after 3 wk, and after 6 wk of treatment. Representative images of 3D-reconstructed tumors are shown, with an untreated WT cerebellum (shown in yellow) displayed for reference. (C) Tumor volumes (mm^3) were estimated at each time point for vehicle-treated ($n = 5$) and saridegib-treated ($n = 7$) $Ptc^{C/C}$ mice. None of the vehicle-treated mice survived until the 6-wk imaging time point.

The MRI images were also used to calculate tumor volumes (see Fig. 3 for representative images of 3D-rendered tumor volumes generated from serial MRI images). This analysis confirmed the significant reduction in tumor volume by 3 wk of saridegib treatment (average tumor volume at enrollment = $1,108 \text{ mm}^3$; average tumor volume after 3 wk of daily saridegib = 580 mm^3 ; $P = 0.0005$) but also showed that not all tumors continued regressing as treatment continued (average tumor volume after 6 wk of daily saridegib = 848 mm^3 ; $P = 0.05$). In contrast, all tumors in vehicle-treated mice continued progressing, with average tumor volumes increasing from $1,082 \text{ mm}^3$ at enrollment to $1,408 \text{ mm}^3$ at the 3-wk time point. MRI volumetrics were additionally validated by 3D tumor volume rendering of serial H&E-stained tissue sections from a cohort of mice analyzed by MRI (Fig. 3). The MRI and histological findings prompted two sets of experiments: one to assess the impact of maintenance treatment regimens on survival and the other to establish the mechanism(s) underlying disease progression during treatment.

Maintenance Saridegib Administration Prolongs Survival. To further establish the extent to which saridegib can prolong survival, we assessed maintenance dosing regimen. Mice were given daily saridegib (20 mg/kg per dose) for 6 wk ($n = 19$) and then either taken off the drug ($n = 6$) or given maintenance dosing (20 mg/kg twice per week) for an additional 6 wk ($n = 13$). Tumors progressed rapidly after the withdrawal of drug after the initial 6 wk of daily treatment (Fig. 5A, light purple), resulting in death within an average of 10 d. In contrast, 53% of mice receiving maintenance dosing (Fig. 5A, dark purple) were still alive at 6 wk after starting twice-a-week therapy. Thus, continued saridegib treatment after 6 wk of daily therapy prolonged median survival fivefold compared with vehicle-treated control animals. Having established tumor regression, neurologic improvement, and a survival advantage conferred to $Ptc^{C/C}$ mice, we next sought to determine whether tumor-initiating capacity, which is important for metastases generation, was impaired by drug treatment.

Saridegib Reduces Medulloblastoma Tumor Initiating Capacity. Medulloblastoma cells from the $Ptc^{C/C}$ mice have tumor-initiating potential, as evidenced by their ability to form new tumors when transplanted to WT recipient mice. Tumors were established from 9 of 11 drug-naïve donors, and 43% (54 of 127) of recipients grew flank tumors. In contrast, the same approach yielded tumors in only 23% (18 of 78) of recipients when donors were treated with daily saridegib for 6 wk (20 mg/kg) before transplantation (Fig. 5B). The difference in tumor take rate indicated that saridegib reduced tumor-initiating potential in this aggressive medulloblastoma mouse model when transplanted in flank ($P = 0.017$). Interestingly, the tumor growth rate in saridegib-treated donor allografts differed from that of the drug-naïve donor group. Flank allografts established from the drug-treated donor group grew much more slowly and often stopped growing. One of six tumors showed spontaneous tumor regression in the absence of drug after initial growth to 895 mm^3 .

Saridegib Induces Regression of Flank Allografts from Drug-Refractory Donors. To explore whether the resistance was through cell-autonomous mechanisms, we used the allograft models to investigate the effect of saridegib treatment on tumor size. When the flank allograft tumor volumes reached $1,000 \text{ mm}^3$, recipient mice received either daily saridegib (20 mg/kg) or vehicle treatment, and the growth of flank allografts was monitored over a 9-wk period. Daily i.p. administration of saridegib into recipient mice suppressed tumor growth to the point that tumors were undetectable in 100% of both allograft groups (Fig. 5C). We attribute the response of flank tumors derived from the saridegib-treated donor mouse to higher drug concentrations in the flank tumors compared with brain tumors, the latter of which are protected by the blood-brain barrier. We found that saridegib concentrations were ~ 10 – 15 -fold higher in flank tumors than in cerebellar tumors at the same dosing regimen (Table S1). Interestingly, the markedly higher drug concentrations achieved in flank tumors were sufficient to overcome the drug tolerance observed in the cerebellar tumor of the donor mouse. However, the higher concentration

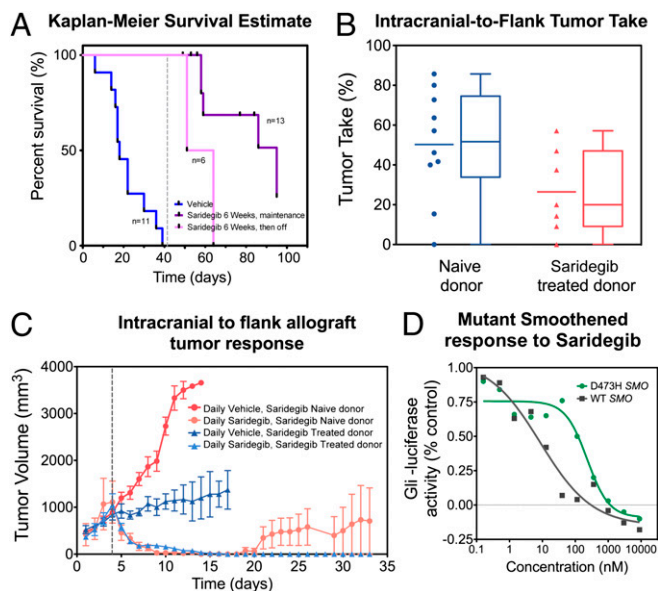


Fig. 5. Saridegib maintenance administration prolongs survival in mice bearing intracranial medulloblastomas, whereas continued saridegib administration induces regression of flank allografts from drug-resistant donors. (A) Three- to five-week-old *Ptc^{CC}* mice symptomatic for medulloblastoma were randomized to receive vehicle (blue line) or saridegib (purple lines). Mice were initially given daily saridegib (20 mg/kg per dose) for 6 wk ($n = 19$) and then taken off the drug ($n = 6$; pink line) or given maintenance dosing (20 mg/kg twice per week) for an additional 6 wk ($n = 13$; purple line). Daily saridegib followed by twice-weekly dosing provided a significant survival benefit compared with vehicle controls ($P < 0.001$) and to mice taken off of the drug ($P = 0.001$). (B) Flank allografts were established in 43% of recipients from drug-naïve *Ptc^{CC}* donors. Only 23% of recipients developed flank tumor when donors were treated with saridegib daily for 6 wk (20 mg/kg) before transplantation. (C) Recipient mice bearing drug-naïve and saridegib-treated allograft tumors were then treated with daily saridegib (20 mg/kg). Dotted line indicates beginning of treatment. Tumors were undetectable in both allograft groups by day 15. Two of five tumors became unresponsive during the 9-wk trial despite initial responses to saridegib. (D) The average Gli-luciferase reporter activity was measured in C3H10T1/2 cells transfected with WT *SMO* (gray) or the D473H *SMO* mutant (green) after treatment with various doses of saridegib. Saridegib inhibited reporter activity at an IC_{50} of 9 nM in C3H10T1/2 cells transfected with WT *SMO* and also showed activity against the D473H *SMO* mutant at an IC_{50} of 244 nM. Reporter activity is normalized to untreated C3H10T1/2 cells. (Error bars: SEM.)

alone was not sufficient to sustain remission in mice that received flank allografts from drug-naïve donors. Two of five tumors progressed while on therapy during the 9-wk trial despite initially disappearing in response to saridegib administration.

Escape from Shh Inhibition Accompanies Tumor Progression in Saridegib-Treated Mice. To better understand drug engagement with Shh pathway activity after prolonged treatment, we assessed the level of *Gli1* inhibition by saridegib at the end of 6 wk of daily therapy. Reduced suppression of Shh signaling at the end of therapy would indicate the emergence of saridegib-resistant cells. This possibility was supported by the observation that saridegib suppressed *Gli1* levels by 83% after 4 d of daily treatment, by 52% after 2 wk of therapy, and by 29% after 6 wk of therapy compared with that of vehicle-treated control tumors (Fig. 6A). The blood-brain barrier has been shown to limit drug penetration into the brain over time through induction of drug efflux pumps (10); this was not the case in our study because saridegib concentrations increased in cerebellar tumors over time (Table S1).

Pgp-Mediated Efflux Transport. One of the main mechanisms of drug resistance in cancer cells is aberrant expression of ATP-

binding cassette (ABC) transporters, which use active transport to efflux drugs from treated cells. Many chemotherapeutic drugs and Shh inhibitors are substrates of the ABC transporter Pgp. To determine whether Pgp was up-regulated in response to saridegib therapy, we quantified Pgp transporter expression via Western blotting in samples from vehicle-treated and saridegib-treated mice. The expression levels of Pgp in tumor homogenates were significantly increased by daily treatment with saridegib for 6 wk (Fig. 6B). We compared the function of Pgp in untreated and saridegib-treated medulloblastomas by using calcein-AM, a fluorescent Pgp substrate that quantitatively measures Pgp activity. Intracellular accumulation of calcein in untreated and saridegib-treated mice was measured by flow cytometry: 79.5% of vehicle-treated tumor cells incorporated calcein compared with only 38.6% of accumulation in saridegib-treated *Ptc^{CC}* tumors (Fig. 6D). The experiment was repeated in the presence of the Pgp inhibitor verapamil. Increase in the intracellular level of fluorescence after exposure to verapamil indicates the presence of Pgp transporters in saridegib-treated *Ptc^{CC}* tumors (Fig. 6C).

To determine whether Pgp inhibition influenced the affect of saridegib on *Gli1* expression, we measured *Gli1* levels in the presence of the Pgp inhibitor verapamil and saridegib. Indeed, inhibition of Pgp transporter via verapamil treatment reversed drug resistance, suggested by decreased *Gli1* levels within tumors receiving the combined therapy (Fig. 6A).

Lack of Resistance-Inducing Mutations or Gli Amplification. Previous studies revealed that *Smo*-activating or drug resistance point mutations occur in transmembrane domains six (TM6) or seven (TM7) (4, 11). In contrast, tumors that grew despite ongoing saridegib therapy showed no evidence of mutations in TM6 or TM7. Of the eight brain and three flank tumors from which the *Smo* gene was sequenced, only one showed sequence variations that could not be readily attributed to known interstrain single-nucleotide polymorphisms. This point mutation at asparagine 223 is not within any of the seven transmembrane domains of the *Smo* protein and does not map to a region of the protein with a known functional domain. We conclude that it is unlikely that the regrowth of both intracranial and flank allografted medulloblastomas depends on de novo *Smo* mutations.

A recent report showed that point mutations were found only infrequently in tumors that developed resistance to the *Smo* inhibitor NVP-LDE225, but *Gli2* amplifications were observed in 50% of resistant tumors (12). PCR analyses of genomic DNA from eight saridegib-resistant brain tumors revealed no *Gli2* amplification. Thus, the cell-autonomous genetic events that lead to resistance to GDC-0449 and NVP-LDE225 were not present in saridegib-treated medulloblastoma tumors, indicating that this cyclopamine derivative interacts with the target protein in a manner distinct from the synthetic Shh inhibitors. Furthermore, array-comparative genomic hybridization (aCGH) showed no focal gains or losses across the entire genome of saridegib-treated tumors compared with normal.

Expression Profiling of Saridegib-Treated Tumors Showed Minor Changes in Shh Pathway Signatures. We used an Illumina microarray to validate mRNA expression signature of vehicle- and saridegib-treated tumors. Using Ingenuity Pathway Analysis, we identified several networks/pathways that were statistically significantly enriched, including those involved in cancer, neurological disease, cell death, and cellular movement (Table S2). The top most-differentially expressed genes are listed in Table S3. We examined the level of 11 gene SHH subgroup signatures: butyrylcholinesterase (*BCHE*); *GLI1*; *GLI2*; inter- α -trypsin inhibitor heavy chain H2 (*ITIH2*); microtubule-associated monooxygenase, calponin and LIM domain containing 1 (*MICAL1*); PDZ and LIM domain 3 (*PDLIM3*); *PTCH2*; *RAB33A*; secreted frizzled-related protein 1 (*SFRP1*); orthodenticle homeobox 2 (*OTX2*); and neurogenin 1 (*NEUROG1*).

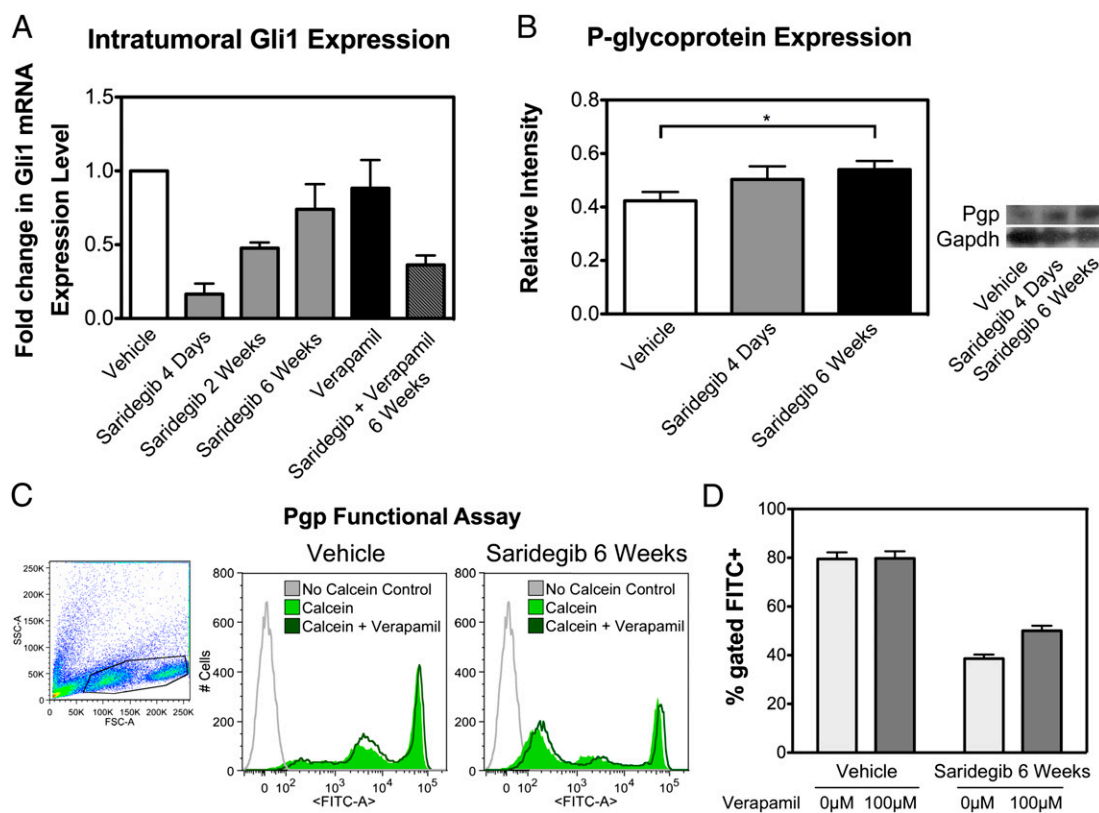


Fig. 6. Mechanisms of resistance in saridegib-treated *Ptc^{C/C}* tumors. (A) The pharmacodynamic activity of saridegib in *Ptc^{C/C}* tumors was confirmed by analysis of *Gli1* mRNA by RT-PCR. Result shows a substantial decrease in *Gli1* expression after 4 d of saridegib treatment ($P = 0.05$). The initial reduction in *Gli1* expression seen in response to daily saridegib (20 mg/kg per dose) was diminished after 6 wk of therapy. Drug resistance to saridegib was partially reversed by cotreatment with the Pgp inhibitor verapamil. Bars represent the average fold change in *Gli1* expression normalized to vehicle-treated controls ($n = 3$). (B) The expression of Pgp was quantified via Western blotting at enrollment, after 4 d, and after 6 wk of treatment. Bars represent the average fold change in Pgp normalized to Gapdh ($n = 3$). (C) Efflux activity of Pgp in saridegib-treated *Ptc^{C/C}* tumors was evaluated by measuring the intracellular fluorescence of calcein by flow cytometry. Compared with vehicle controls, saridegib-treated tumors had lower calcein accumulation. Inhibiting the Pgp activity with 100 μ M verapamil increased calcein fluorescence, as indicated by a small shift of the peak to the right. Gray line indicates autofluorescence of the cells that were not exposed to calcein-AM. (D) Percentage of cells appearing within the FITC⁺ gate was quantified. Pgp-mediated efflux activity was significantly increased in *Ptc^{C/C}* tumors treated with saridegib ($n = 3$). (Error bars: SEM.)

Recurrent tumors showed characteristics of the Shh subgroup similar to the vehicle-treated group (Fig. S3). Among those genes, SFRP1 and OTX2 showed statistically significant differential expression in the drug-treated group compared with that of vehicle-treated group.

Saridegib Activity on D473H *SMO* Mutant. Saridegib was assayed alongside other Smo inhibitors in the C3H10 differentiation assay as previously described (7). Saridegib and inhibitors GDC-0449, LDE225, and SANT-1 all have activity in the 7–30 nM EC_{50} range. Cyclopamine is less potent with an EC_{50} range of 500 nM to 1 μ M. To determine the ability of saridegib to suppress Shh signaling in the context of the D473H *SMO* mutant known to confer resistance to the Shh pathway antagonist GDC-0449 (4), we measured the IC_{50} of saridegib required to inhibit Gli-luciferase activity (Fig. 5D). Saridegib inhibited reporter activity at an IC_{50} of 9 nM in C3H10T1/2 cells transfected with WT *SMO* and also showed activity against the D473H *SMO* mutant at an IC_{50} of 244 nM. Saridegib induced greater than 95% inhibition at 1 μ M concentration in D473H *SMO* mutant cells, which compares favorably with GDC-0449 (3% inhibition at 1 μ M concentration), cyclopamine (the parent drug from which saridegib is derived, 48% inhibition at 1 μ M concentration), and other drugs screened for activity against this mutation (13). These findings are in contrast to results obtained with other Hedgehog pathway antagonists and suggest that saridegib retains

the ability to impair downstream Hedgehog signaling even in the presence of some activating *SMO* mutations.

Discussion

Medulloblastoma is an aggressive malignant brain cancer that is particularly difficult to cure in the recurrent disease setting. Conventional therapies for medulloblastoma impose unacceptable toxicities on children with this disease, and more effective, less toxic alternatives are critical for future care. Smo inhibitors show promise for targeting Shh-driven tumors, but resistance emerges rapidly (4, 5, 13). Because this pathway is considered crucial for several cancer types, efforts are under way to advance drugs that are less prone to resistance induction.

In this study, 6 wk of daily saridegib treatment resulted in 100% survival compared with 0% in the vehicle-treated medulloblastoma-bearing mice. Additionally, a substantial resolution in clinical symptoms was observed in the majority of saridegib-treated mice, secondary to reduced hydrocephalus and calvarial swelling and accompanied by increased mouse activity. Treatment with saridegib sharply reduced tumor allograft engraftment success, and some allografts established from saridegib donors underwent spontaneous regression after initial significant growth. Both observations are consistent with the notion that Smo inhibitors limit medulloblastoma tumor-initiating capacity.

This study is important because it examines Hedgehog pathway antagonism in the conditional *Ptc^{C/C}* mice. A previous study

demonstrated the efficacy of the HhAntag Hedgehog antagonist in a less aggressive *Ptch1*^{+/-}; *p53*^{-/-} model of medulloblastoma arising in the *Ptch1* heterozygous, *p53*-null background (3). Although these results share similarities to our current study, an important contrast must be noted in the extent of tumor burden in response to heterozygous versus homozygous loss of *Ptch1* within the cerebellum. In the *Ptc*^{C/C} model, all cerebellar granule neuron precursor cells are lacking the inhibition normally mediated by the *Ptch1* receptor, and tumor formation is early, aggressive, and uniform throughout the cerebellum. Thus, the response to saridegib was remarkable given the continuous source of neoplastic cells and the extent of initial tumor burden in intracranial *Ptc*^{C/C} tumors.

The heptahelical structure of the Smo receptor is required for binding of cyclopamine and is targeted by G protein-coupled receptor modulators (14), and mutations near the highly conserved transmembrane domains can reduce the affinity of compounds specifically targeted to this binding pocket. In contrast to the previous report of mutation-based resistance to GDC-0449, we did not observe mutations in the TM6 or TM7 domains of the *Smo* allele, nor did we observe *Gli2* amplification.

Gene expression profiling suggests minor alteration of two Shh signature genes in the saridegib-treated group. We found down-regulation of SFRP1 genes and up-regulation of OTX2. Previously, SFRP1 has been identified as a prime biomarker for the Shh subgroup (15), and a high expression level of SFRP1 was found in *Ptch1*^{+/-} tumors (16). The expression of OTX2 is low or absent in Shh-driven human medulloblastoma (17, 18). OTX2 copy number gain has been associated with more aggressive tumor phenotypes and decreased patient survival (18), and inhibition of OTX2 in medulloblastoma cell lines decreased tumor proliferation and formation in vitro (19). It is currently unclear whether modest up-regulation of OTX2 is related to saridegib resistance.

The absence of genetic mutations in *Smo* or amplifications of *Gli2* raises the question of why tumors eventually grow in mice treated with saridegib. It is possible that it is a reflection of the highly aggressive model, in which most cells in the granule cell lineage completely lack negative regulation of the mitogenic Shh pathway. Alternatively, saridegib activity could be affected by common drug resistance mechanisms, such as ABC transporters. Indeed, we saw increased Pgp expression in the brain tumors of mice treated for 6 wk with saridegib (Fig. 6). Furthermore, co-administration of verapamil, a Pgp inhibitor, partially restored the capacity of saridegib to reduce *Gli1* even after extended (6-wk) treatment periods. A Pgp functional assay with calcein-AM revealed increased level of efflux activity in saridegib-treated *Ptc*^{C/C}. The relationship between Pgp and saridegib activity is

somewhat confusing because the binding site of cyclopamine, and presumably the cyclopamine derivative saridegib, lies on a portion of Smo that is internal to the plasma membrane. In addition, it is not clear whether the drug accesses the binding site from the cytoplasmic side or the surface of the plasma membrane.

Unlike studies of other oncology drugs, including cytotoxic chemotherapy agents, our results are unique because they show a fivefold increase in survival in mice with advanced, aggressive, autochthonous brain tumors. Our nonclinical studies clearly demonstrate the efficacy of saridegib in resolving clinical symptoms of advanced medulloblastoma and prolonging survival in the *Ptc*^{C/C} model.

Materials and Methods

Mouse Models and Drug Dosing. Animal experiments were conducted in accordance with National Institutes of Health and institutional guidelines. Conditional *Ptc*^{C/C} mice were generated by breeding mice homozygous for the floxed *Ptch1* allele (20) to *Math1*-Cre mice (8). For allograft studies, medulloblastomas from symptomatic *Ptc*^{C/C} mice were harvested, triturated, filtered, and resuspended in equal parts of DMEM and Matrigel (BD Biosciences). Then, 1×10^6 cells were injected s.c. into the flank of WT littermates. Tumor volume was calculated from caliper measurements ($0.5 \times \text{length} \times \text{width}^2$). P21 to P36 *Ptc*^{C/C} mice were randomized to receive either saridegib (20 mg/kg per dose; Infinity Pharmaceuticals) or vehicle control [5% (vol/vol) (2-hydroxypropyl)- β -cyclodextrin (HPBCD); Sigma-Aldrich] administered via daily i.p. injection. Saridegib drug levels in tumor and brain samples were determined as previously described (21). For combination therapy, the ABC transporter inhibitor verapamil (15 mg/kg per dose; Sigma-Aldrich) was administered weekly via oral gavage between the third and sixth weeks.

DNA Sequencing Analysis. DNA was extracted from each sample with the QIAamp DNA Mini Kit (Qiagen). PCR primers were tagged with M13 forward or M13 reverse. Information on primer sequences for SMOOTHENED (SMO) exons 1–12 can be found in Table S4. PCRs were run on a Dyad DNA Engine (MJ Research/Bio-Rad) using the following conditions: 95 °C for 5 min followed by 35 cycles of 95 °C for 30 s, 60 °C for 30 s, 68 °C for 45 s, and then 68 °C for 10 min. Target sequence was sequenced by the Sanger method (GeneWiz) in both forward and reverse directions.

Additional detailed materials and methods are described in *SI Materials and Methods*.

ACKNOWLEDGMENTS. We thank Kerrie Faia, Nigel Whitebread, Mark Stroud, Joyoti Dey, Jeff Delrow, and Sunil Hingorani for assistance. Saridegib (IPI-926) was provided by Infinity Pharmaceuticals. This work was supported by National Institutes of Health Grants R01 CA112350-04 and R01 CA135491-03, Infinity Pharmaceuticals, the National Health and Medical Research Council of Australia, Bear Necessities Pediatric Cancer Foundation, the St. Baldrick's Foundation, the John Trivett Foundation, and Seattle Children's Hospital Brain Tumor Endowment.

- Rossi A, Caracciolo V, Russo G, Reiss K, Giordano A (2008) Medulloblastoma: From molecular pathology to therapy. *Clin Cancer Res* 14:971–976.
- Katoh Y, Katoh M (2009) Hedgehog target genes: Mechanisms of carcinogenesis induced by aberrant hedgehog signaling activation. *Curr Mol Med* 9:873–886.
- Romer JT, et al. (2004) Suppression of the Shh pathway using a small molecule inhibitor eliminates medulloblastoma in *Ptch1*^{+/-}*p53*^{-/-} mice. *Cancer Cell* 6(3):229–240.
- Yauch RL, et al. (2009) *Smoothed* mutation confers resistance to a Hedgehog pathway inhibitor in medulloblastoma. *Science* 326:572–574.
- Rudin CM, et al. (2009) Treatment of medulloblastoma with hedgehog pathway inhibitor GDC-0449. *N Engl J Med* 361:1173–1178.
- Metcalfe C, de Sauvage FJ (2011) Hedgehog fights back: Mechanisms of acquired resistance against *Smoothed* antagonists. *Cancer Res* 71:5057–5061.
- Tremblay MR, et al. (2009) Discovery of a potent and orally active hedgehog pathway antagonist (IPI-926). *J Med Chem* 52:4400–4418.
- Yang Z-J, et al. (2008) Medulloblastoma can be initiated by deletion of *Patched* in lineage-restricted progenitors or stem cells. *Cancer Cell* 14(2):135–145.
- Veisoh M, et al. (2007) Tumor paint: A chlorotoxin: Cy5.5 bioconjugate for intraoperative visualization of cancer foci. *Cancer Res* 67:6882–6888.
- Löscher W, Potschka H (2005) Drug resistance in brain diseases and the role of drug efflux transporters. *Nat Rev Neurosci* 6:591–602.
- Taipale J, et al. (2000) Effects of oncogenic mutations in *Smoothed* and *Patched* can be reversed by cyclopamine. *Nature* 406:1005–1009.
- Buonamici S, et al. (2010) Interfering with resistance to *Smoothed* antagonists by inhibition of the PI3K pathway in medulloblastoma. *Sci Transl Med* 2:51ra70.
- Dijkgraaf GJ, et al. (2011) Small molecule inhibition of GDC-0449 refractory *Smoothed* mutants and downstream mechanisms of drug resistance. *Cancer Res* 71:435–444.
- Chen JK, Taipale J, Cooper MK, Beachy PA (2002) Inhibition of Hedgehog signaling by direct binding of cyclopamine to *Smoothed*. *Genes Dev* 16:2743–2748.
- Northcott PA, et al. (2011) Medulloblastoma comprises four distinct molecular variants. *J Clin Oncol* 29:1408–1414.
- Pei Y, et al. (2012) An animal model of MYC-driven medulloblastoma. *Cancer Cell* 21(2):155–167.
- Di C, et al. (2005) Identification of OTX2 as a medulloblastoma oncogene whose product can be targeted by all-trans retinoic acid. *Cancer Res* 65:919–924.
- Adamson DC, et al. (2010) OTX2 is critical for the maintenance and progression of Shh-independent medulloblastomas. *Cancer Res* 70(1):181–191.
- Bunt J, et al. (2010) Regulation of cell cycle genes and induction of senescence by overexpression of OTX2 in medulloblastoma cell lines. *Mol Cancer Res* 8:1344–1357.
- Adolphe C, Hetherington R, Ellis T, Wainwright B (2006) *Patched1* functions as a gatekeeper by promoting cell cycle progression. *Cancer Res* 66:2081–2088.
- Olive KP, et al. (2009) Inhibition of Hedgehog signaling enhances delivery of chemotherapy in a mouse model of pancreatic cancer. *Science* 324:1457–1461.